IIASA

International Institute for Applied Systems Analysis • A-2361 Laxenburg • Austria
Tel: +43 2236 807 • Fax: +43 2236 71313 • E-mail: info@iiasa.ac.at • Web: www.iiasa.ac.at

INTERIM REPORT IR-98-044/July

Land cover in the Horqin Grasslands, North China. Detecting changes between 1975 and 1990 by means of remote sensing.

Sara Brogaard (sara.brogaard@natgeo.lu.se)
Sylvia Prieler (prieler@iiasa.ac.at)

Approved by
Günther Fischer (fisher@iiasa.ac.at)
Leader, *Land Use Change Project*

Contents

List of Figures and Tables

Abstract

This paper aims to identify land cover changes of the western part of the Horqin steppe by means of Landsat MSS satellite data. The Horqin steppe is located in the temperate semi-arid zone of North China, Inner Mongolia Autonomous Region. The steppe is considered to be one of the most drastic examples of land degradation in China's semi-arid region.

Two Landsat MSS scenes, one for the year 1975, the other for 1989, with an overlapping area of around 20000 km^2 were used for the land cover change detection. After performing geometric and radiometric corrections, an unsupervised cluster classification revealed six major land cover classes including water. Then a supervised Maximum Likelihood classification was applied to both scenes using the results from the unsupervised classification as well as the Horqin desertification/land use map (Lanzhou Institute of Desert Research, 1991) and filed data, which have been collected in September 1996. 5-10 training areas for each class where identified for the five land cover classes: (1) Moving sand with less than 10% vegetation cover, (2) farmland, (3) grassland with a vegetation cover of 10-60%, (4) grassland with a vegetation cover of 60-100% and (5) scrub forest. Further a post classification filtering process was applied to produce more homogenous areas. Finally by means of visual interpretation and a digital elevation model obvious misclassifications, such as overrepresentation of cropland at the expense of scrub forest or grassland with vegetation cover >60%, were changed.

A comparison of the 1989 image classification with the collected field data gave poor results. Most likely this is due to the time difference between image acquisition and field data but also the result of low precision when georeferencing the image. Another source of error could be the actual sampling method, which has occurred close to river systems, where land use and land cover may undergo rapid changes.

Comparing the 1975 and 1989 final classifications three main types of changes may be observed. First, larger areas of farmland are found in the 1989 image compared to 1975, mainly distributed around the Xiliao River system. Second a significant area of the class 'grassland with 10-60% vegetation cover' in 1975 has become converted to the class 'grassland 60-100% vegetation cover' by 1989. Third, sandy surfaces with the lowest vegetation cover, <10% have also decreased. Therefore this study does not confirm any overall degradation of the area as far as concerns vegetation cover. On the contrary, the study implies a possible improvement of grassland, especially in the loess area south of the Xilao River. Precipitation data seem not to explain these changes. However, additional data including monthly precipitation data should be analyzed.

Acknowledgments

The authors wish to thank the colleagues of the IIASA Land Use Change (LUC) project for their support at different stages during the work. We especially appreciated the comments, advice and help of Günther Fischer and Xiubin Li, who were most involved in this work. We would further like to thank Ulf Helldén, from the University of Lund, for his support in obtaining the remotely sensed images and his comments on this study.

The participation of Sara Brogaard was financed by the Swedish National Member Organization of IIASA, FRN (Forsknings Råds Nämden), through the 1997 YSSP program.

About the Authors

Sara Brogaard joined the Land Use Change project as a participant of IIASA's Young Scientists Summer Program in 1997. Sara is a Ph.D. student from the Department of Physical Geography, University of Lund, Sweden.

Sylvia Prieler is a Research Scholar and GIS specialist working with the Land Use Change project at IIASA.

Land cover in the Horqin Grasslands, North China. Detecting changes between 1975 and 1990 by means of remote sensing.

Sara Brogaard and Sylvia Prieler

1. Introduction

The IIASA project "Modeling Land Use and Land Cover changes in Europe and Northern Asia (LUC)" was established in 1995, with the objective of analyzing the spatial characteristics, temporal dynamics, and environmental consequences of land-use and land-cover changes which have occurred in Europe and Northern Asia over the period of 1900 and 1990 as a result of a range of socio-economic and biogeophysical driving forces. The analysis is used to project plausible future changes in land use and land cover for the period 1990 to 2050 under different assumptions of future demographic, economic, technological, social and political development (Fischer *et al.* 1996*)*. Previous and ongoing case studies and modeling approaches within the LUC project have been based on existing land use/cover databases of different scales and resolutions.

The objective of the study presented in this paper is to evaluate the usefulness of digital analysis of Landsat MSS satellite data for identification of broad land cover changes of the western part of the Horqin steppe, Inner Mongolia Autonomous Region. The Horqin steppe is located in the temperate semi-arid zone of North China. Over the past decades changes in the agricultural production system have caused land cover changes including desertification. The steppe is considered to be one of the most drastic examples of land degradation in China's semi-arid region. In the study area two processes of land cover changes are of particular importance:

- conversion of grassland to cultivated land
- changes in the density of vegetation cover, a process which rather falls under the concept of land cover modification

The analysis of Landsat MSS data of the Horqin area is part of a project sponsored by the Swedish Space Board under the project: "Land cover, climate and desertification in the

drylands of China" – a study of change for a sustainable land use. Since it is of interest for IIASA to incorporate remote sensing analysis into the LUC project research, it was decided to undertake an initial analysis of this data set within the IIASA Young Summer Scientist Program. For this study two Landsat MSS scenes were chosen, one for the year 1975, the other for 1990, with an overlapping area of around 20 000 km^2. The results of the study will be used as guidance for further analysis of the remaining data set covering the Horqin steppe.

2. The Horqin Steppe

2.1 Location

The Horqin steppe is located in the northeastern part of China. The main part of the steppe belongs to Inner Mongolia Autonomous Region but also parts of Jilin and Liaoning provinces. The area included in this study is around 20 000 km^2, located between 42°20 to 44°00 N latitude and 118°30 to 120°50 E longitude in the western part of the Horqin steppe mainly falling within the Chifeng City Prefecture, Inner Mongolia (Figure1).

Fig. 1. The position of the study area in the northeastern part of China, Inner Mongolia Autonomous Region.

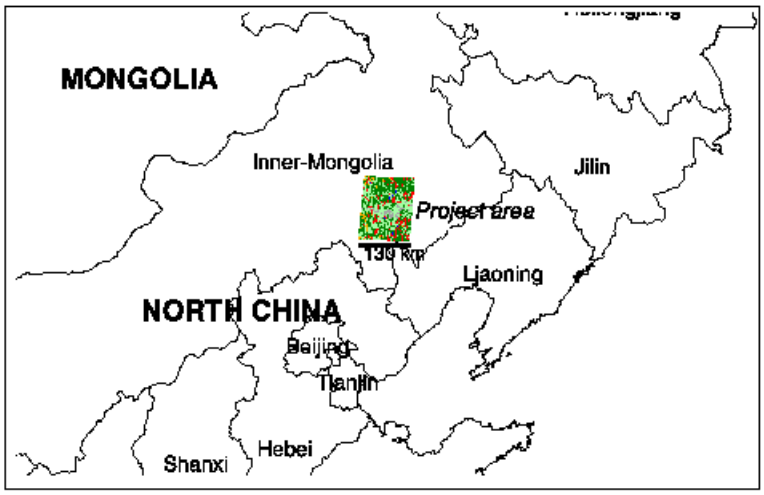

2.2 Climate

The region belongs to the continental temperate semi-arid zone. Winter is usually cold and dry while summer is generally warm and wet. Annual mean temperature is 6°C and annual precipitation around 400mm, increasing from the plain in the southeast towards the mountainous areas in the north west. The precipitation of the growing season (April to September) makes up about 90% of the total annual precipitation and the variation

between years is large (Zhu et al. 1988). Rainfall is the limiting factor for the natural vegetation during the growing period. Figure 2 shows precipitation data at Linxi rainfall station (43°36 N, 118°04 E) which is located in the project area. For the period 1936 to 1988 no trend is evident. A complementary time series from the Naiman station (43°06 N, 121°15 E) east of the study area until 1990 is presented in Figure 3. A trend towards higher variability is apparent. When looking more specifically at the years 1975 and 1989 it can be concluded that precipitation in these years has been slightly below average. The similar situation of rainfall facilitates land cover comparison between the two years.

Fig 2. Linxi rainfall station 1936-1988. a) Precipitation b) Deviation from mean precipitation for the period.

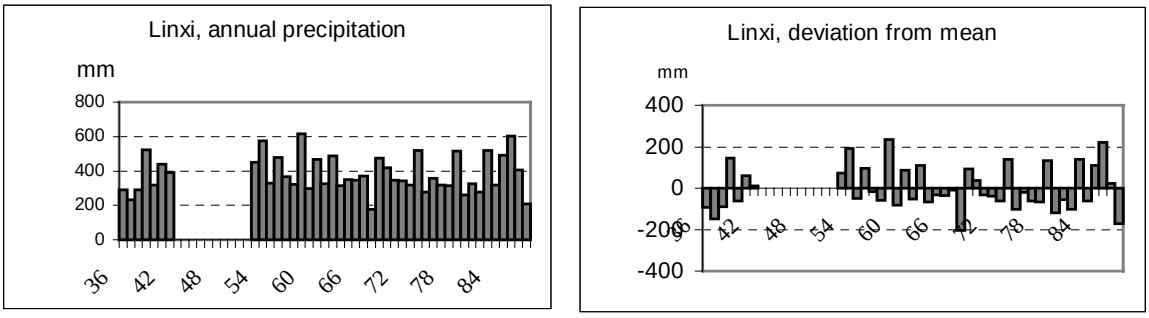

Figure 3. Naiman rainfall station 1969-1990. a) Precipitation b) Deviation from mean precipitation for the period

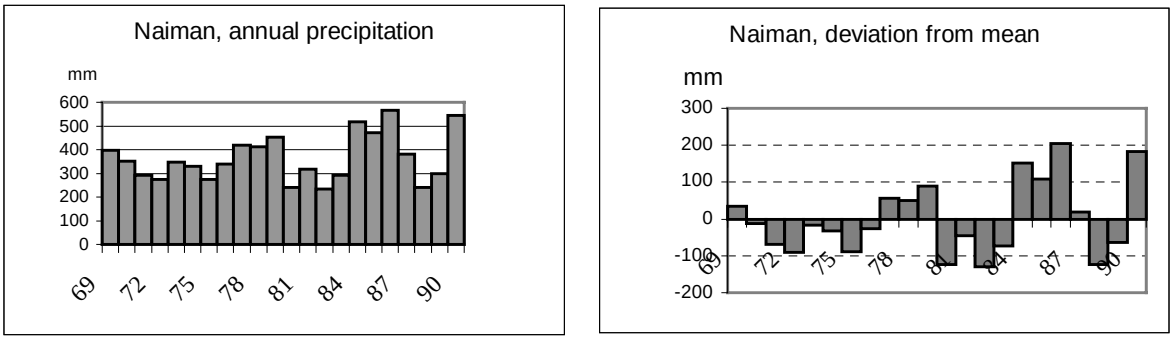

2.3 Geomorphology and soils

The Xiliao River plain makes up the major part of the Horqin steppe and is also referred to as Horqin Sandy Land. It consists of alluvially deposited sediments with decreasing grain size from the east to the west, reflecting the flow direction of the water system and the local wind regime. This originally alluvial material has been reformed through wind action, and now makes up the vegetated and unvegetated dunes which forms the landscape of the Xiliao river Plain. To the west the area is bordered by mountains and to

the south by loess hills (Zhu *et al.* 1988). The east to west sequence of soil zones on the Horqin Plain is temperate forest steppe black soil, meadow steppe chernozems, steppe castanozems, semi-desert brown calcareous soil and desert soils. The distribution pattern of these soils are also influenced by changes in elevation of adjacent mountains (National Research Council 1992).

2.4 Vegetation and land use

According to the regional vegetation map of China the Horqin steppe belongs to the temperate steppe region, which is divided into two zones, forest meadow zone and the typical steppe zone. The latter, dominating in the study area, is characterized by soils with lower organic matter content, lower production of forage and cultivated crops and also lower population density. Vegetation of the typical steppe includes *Aneurolepidium chinese*, *Stipa grandis* and *Agropyron michnoi* (US National Research Council 1992). The vegetation of the degraded dune areas consists mainly of scrub as *Artemisia Halondendron*, *A. scoparia* and *Caragana microphylla* and grasses as *Digitaria ischaemum* and *Setaria viridis* (Xeuyoung 1992). Land use in the area can be classified into semi-farming and semi-nomadic in the marginal zone of dry-farming and animal grazing (Zhu *et al.* 1988). Maize, wheat, beans, and rice in the river valleys, are the dominating crops. The livestock population mainly consists of sheep and cattle (Zhao personal communication).

2.5 Land degradation

In previous studies of the semi-arid parts of China, the human factor is often stressed as the major driving force for land degradation. Sheehy (1994) describes the development of China's arid regions in relation to the agricultural practices in the rest of the country. In humid and sub-humid China, irrigated and rainfed sedentary agriculture was feasible and became the basis for the cultural and political system. In the semiarid and arid steppe the low annual precipitation and cold temperatures prevented the development of sedentary agriculture except in a few scattered locations. Extensively managed production systems characterized by grazing animals with relatively high mobility formed the basis of agricultural production on steppe grazing land. The political and cultural systems which developed in accordance with the mobile production system of the steppe were in disaccord with political and cultural systems of agricultural China. Sheehy (1994) claims that this made the ecotone between semi-arid steppe grazing land and the sedentary agriculture of sub humid China a tension zone throughout much of the recorded history of North China, where desertification has had an extended historical precedence. Sedentary agriculture was often used as a means to consolidate Chinese political, social, and military goals. The land use pattern was cultivation of grassland, subsequent abandonment following misuse of water resources, overcultivation, overgrazing, or translocation of people to where the process could be repeated. The steppe vegetation recovered to natural condition if sufficient time passed and the human activities were lightened.

The land use pattern described above is identified in the historical records of the Horqin steppe. The natural land cover of the area is considered to be temperate tree scattered rangeland. According to Li (1990) the population of the region began to increase several centuries ago when a significant movement of Han agriculturists into the area started. Most of the good chernozem soils were converted to cropland and also marginal land was put under cultivation. The area available for grazing was reduced. A large influx of people, expansion of agriculture, reduction of grazingland and increase in livestock numbers have degraded vegetation throughout this region and left land bare in many areas. Zhu *et al.* (1988) considers the human impact particularly marked since the 1949 revolution when population expansion and the new ideas of productivity all lead to desertification of the area, which can not be compared with human action in the past. After the collapse of the Great Leap Forward in the late 1950´s the "grain first" policy was introduced. The policy called for maximum local self-sufficiency and lead to over reclamation and desertification of the sandy grasslands (Smil 1987). According to Ma and Chang (1980, in Smil 1987) about 65 000 km^2 of farmland and grassland became desertified during the period of 1949 and 1980, with nine-tenths of the loss ascribed to improper land use, mostly conversion of semi-arid grassland to grain field and overgrazing. Another estimation made by Lanzhou Institute of Desert Research in 1986, when the institute was under the direction of Prof. Zhu Zhenda, concluded that China's deserts have been expanding at the rate of 1000 km^2 per year during the past half century. In all, 176 000 km^2 of land in north China have been classified as desertified (National Research Council 1992).

The situation which has existed in the pastoral areas of China since the 1978 economic reforms is, according to Longworth and Williamson (1993), largely influenced by three broad sets of policy-related issues: population pressures, market distortions and institutional uncertainties. These have been interacting with the adoption of technology in a unique environmental setting to generate development outcomes as well as encouraged rangeland degradation. Smil (1987) on the other hand, states that the previous policies as "grain first" were officially abolished with the new political orientation since 1987. Conversion of grassland and forests into cropland became strictly regulated and many of the most offensive forms of land degradation have been reduced and in many cases even eliminated.

3. Remote sensing and applications to arid environments

Remote sensing is a collective name for several techniques which study at distance the ground surface or the atmosphere. Sensors installed on satellites or airplanes receive and/or send radiation to the earth. The variation in amount and wavelength of the reflected energy between studied objects or phenomena gives the object its spectral signature and makes it possible to distinguish between different types of land use, vegetation, soils etc. Figure 2 exemplifies the reflectance characteristics of green vegetation and dry soil in the visible and near infrared wavelength bands and the channels 1-4 of Landsat MSS (Multispectral Scanner). The reflectance of vegetation is in the visible part of the spectrum dominated by strong absorption due to chlorophyll and other

pigments in the plant. Radiation in the red and blue wavelengths are more strongly absorbed than the green wavelengths, resulting in a small peak in the green band. In the near infrared region the reflection is increasing considerably due to the internal structures of the plant. The relation between the red and near infrared reflectance are used for quantification of biomass by a number of vegetation indices (Hoffer 1978).

Figure 4. Spectral reflectance of dry soil and green vegetation. The four channels of Landsat MSS are indicated; the green, the red and two infrared channels (modified after Lillesand and Kiefer 1995).

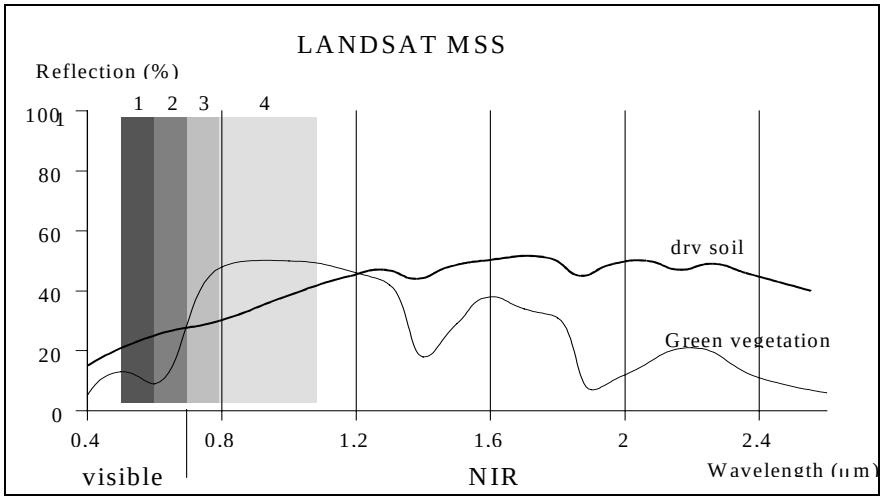

Landsat and SPOT data have found widespread use in agricultural land cover studies in semi-arid environments. The application involves both visual and/or computer assisted interpretation techniques, and it may be based upon single satellite images or on time-series of images from different seasons or years. If the area to be studied is relatively large, satellite images will often be an inexpensive alternative to traditional sources, presuming that the ability to handle the data is already established. Results tend to be the most reliable in areas with the following properties: simple land use pattern with few crops, good spectral contrast between crops and natural vegetation, flat, good chances of cloud-free days during the growing season, relatively large and rectangular fields or clusters of fields with distinct boundaries (Rasmussen 1993). Regarding biomass production on pastures, it has been demonstrated that it is difficult to apply high-resolution satellite images from the Landsat and Spot series because sometimes extremely high natural within- and between-year variability tend to obscure any long-term trends in vegetation cover (Ahlcrona 1988, Rasmussen 1993).

Major mapping of the north China drylands has been done within the program of "Combating Desertification in China". Objectives included an identification of areas at risk for desertification and the compilation of so-called desertification maps. Within this program the Map of Desertification in Horqin Grassland at a scale of 1:500 000 (Lanzhou Institute of Desert Research, 1991) including the classes latent, slight, moderate and severe was produced. Also land use and geomorphologic features are indicated on the

map. The map is based on visual image interpretation of aerial photographs and satellite images, evaluation of physical and socio-economic data and field monitoring and investigations. Vegetation cover, identified by the remotely sensed data and field investigations, is the variable given the largest weight. Zhu *et al.* (1988) (summarized in Bremborg 1996) describes the typical vegetation status within the different desertification degree classes. Latent desertified land is characterized by dense, mostly perennial, vegetation and unaffected topsoil. A variety of plant species that may be used for livestock fodder as *Artemesia halodendron*, *Cargana microphylla*, and *Hedysarum fruticosum* characterizes this class. The slightly desertified land is similar to the latent class but with less dense complement of perennial spieces. In the moderate desertified class the vegetation density decreases further and annual variation is great, as 60-70 % of the biomass consist of annual plants as *Setaria viridis*. The severely desertified land has lost all its utilization value. Vegetation cover is less than 10 % and scattered on the dunes and in the inter dune depressions. Plant species include *Agriophyllum squarrosum* and *Salix gorgejevii*.

Luk (1983) made a study on the mobile sand-dune distribution in order to identify the general trend of desertification in the Maowusu desert, situated in the bend of the Yellow River in Shaanxi and Inner Mongolia provinces, over the period 1953 to 1976. Aerial photographs from 1945, various map sources and Landsat MSS satellite images from 1974-1978 were used. Luk claims that throughout the period desert expansion occurred, but with rates varying over time and space. Rapid desertification was observed during 1959-63 and 1971-76. Desertification rates were compared with precipitation and land use information. The conclusion of the study was that droughts had only accentuated the process, while the primary cause of desert expansion was attributed to excessive clearing of land for rain-fed agriculture as well as overgrazing.

4. Satellite data and preprocessing

Two Landsat MSS scenes from 1975 and 1989 were used for the land cover change detection (Table 1). The MSS sensor consists of detectors, which produce signals proportional to the average amount of light reflected from an area 80x80 meters, which is the geometrical resolution of a Landsat MSS scene. The spatial extension of one scene is 185x185 km and the interval between the registrations is 16 days. The MSS sensor detects the electromagnetic radiation in four channels corresponding to the green and red wave lengths in the visible part of the spectrum, and two channels in the near infrared part (Figure 4).

Table 1. Satellite data used in the study.

Date	Scene row/path	Mission-Sensor	Receiving station
10 June 1975	132/30	Landsat-2 MSS	EROS, USA
20 June 1989	122/30	Landsat-5 MSS	RESTEC, Japan

4.1 Geometric Correction

Raw digital images usually need to be corrected for geometric deformation due to variation in altitude, velocity of the sensor platform, for variations in scan speed and in the sweep of the sensor's field of view, earth curvature, relief displacement etc. The systematic errors are normally corrected for at the receiving station. Random distortion needs to be corrected for by the analyst through selection of sufficient number of ground control points (GCP's) with correct coordinates, usually from a map or GPS (Global Positioning System) points, which can be localized in the satellite image. A transformation function is calculated to determine the distorted image positions corresponding to the correct map positions: an undisturbed output grid is defined. In a chosen resampling scheme each cell in this new grid is assigned a gray level according to the corresponding pixel in the original image.

In this study two images were analyzed and adjusted to each other and to the Conical Conformal map projection of the Tactical Pilotage Chart 1:500 000. Table 2 lists the type of corrections done and the evaluated root mean square in pixels. Using the nearest neighbor resampling method a synthetic pixel value in the output image is assigned on the basis of the closest pixel in the input image. The poor accuracy of the image to map transformation of 3- 4 pixels (one pixel 70x70 m) is due to the small scale of the reference map. Maps of larger scale are however difficult to obtain outside China.

Table 2. Geometric correction; number of ground control points, type of resampling method and root mean square (unit pixel) for the corrected scenes.

corrected scene	No of GCP´s	resampling scheme	RMS x	RMS y
1975 scene to 1990 scene	26	2:nd order nearest neighbor	0.93	0.50
1990 scene to map	19	2:nd order nearest neighbor	4.21	3.22

4.2 Radiometric correction

Two main procedures are required in the radiometric correction. The absolute radiometric calibration maintains the relationship between the radiance and the signal output of the detectors and is performed at the receiving station. The relative radiometric calibration is done to compensate for detector-detector, band-band and time-time variations and should therefore be done prior to multi temporal image analyses but also when rationing wavebands (Markham and Baker 1986). The relative radiometric calibration includes the conversion of digital numbers to spectral radiance, which requires post-calibration coefficients, which are specific for the receiving station (Equation 1) (Table 3).

$$L\lambda = Lmin\lambda + \frac{(Lmax\lambda - Lmin\lambda)}{DN\ max} \times DN \qquad (1)$$

where:

DN	=	Digital number on computer compatible tape
DN max	=	Maximum digital number
Lmin λ	=	Minimum spectral radiance
Lmax λ	=	Maximum spectral radiance
L λ	=	Spectral radiance

The next step in the correction procedure is to compensate for sun angle and irradiance effects to calculate the at-satellite reflectance (Equation 2).

$$\rho p\lambda = \frac{\pi \cdot L\lambda \cdot d^2}{Esun\lambda \cdot \cos\Theta s} \qquad (2)$$

where:

ρpλ	=	Unitless effective at-satellite reflectance
L λ	=	Spectral radiance
d	=	Earth - sun distance in astronomical units
Esun λ	=	Mean solar exoatmospheric spectral irradiance
Θs	=	Solar zenith angle in degrees

Table 3. Calibration coefficients (from RESTEC, EROS and astronomical almanac).

Platform	MSS Band	Lmin λ	Lmax λ	Esun	DN max	d	Θs
Landsat 2	1	1.0	21.0	185.6	127	1.01524	31
EROS	2	0.7	15.6	155.9	127	-	-
	3	0.7	14.0	126.9	127	-	-
	4	0.5	13.8	90.6	63	-	-
Landsat 5	1	0.34	20.48	184.9	127	1.01614	31
RESTEC	2	0.48	16.60	159.5	127	-	-
	3	0.43	12.21	125.3	127	-	-
	4	0.44	12.68	87.03	127	-	-

Finally, corrections for the atmospheric effects (i.e. atmospheric radiance and background radiance) must be completed. As meteorological data, atmospheric data and knowledge about background reflectance are normally not available, the haze removal method or the standardization method are commonly used to suppress the effect of sky light and haze (Hall-Kynöves 1988).

In this study the lowest reflectance value was obtained by calculating statistics from six areas of different water bodies within the scene. Lowest values of each wavelength band were found in a hydropower/irrigation dam of the 1975 scene. A subtraction of the difference between this value and the lowest value of the same area in the 1989 scene was made for each band. These difference values amount to 13, 11, 6 and 10 for band 1-4 respectively. Since the same value is used as a standard over the whole scene it is assumed that similar atmospheric conditions exist over the whole scene.

5. Classification methodologies

Image classification can be done manually, by visual interpretation of the data, or digitally where numerical procedures, usually statistically based decision rules, automate the classification process. While a manual classification is superior in the interpretation of spatial information (textural and contextual information), computers can handle the spectral information more efficiently. Although contextual and textural classification algorithms exist the conventional digital classifiers are entirely based on spectral pattern recognition. Normally a multispectral data set is used for the classification as the dimension of the spectral feature space increases with the number of wavelength bands included in the analysis.

The land cover classification chosen in this study is limited to a few major classes according to the limited temporal and spatial resolution of the satellite data and to enable comparison with existing land cover data sources. The latter consist of the Map of desertification in Horqin Grassland and field data collected during September 1996. Prior to supervised classifications an unsupervised cluster classification was applied. Thereafter two classification procedures were combined; the maximum likelihood algorithm and manual classification.

5.1 Cluster classification

Unsupervised classification techniques uncover the major land cover classes that exist in the image, without prior knowledge of what they might be. They are useful for determining the spectral class composition of the data prior to detailed analysis by the methods of supervised classification. Cluster classifications search for clusters of pixels with similar reflectance characteristics in a multi-band image. They also generalize land cover of the image since they are concerned with uncovering the major land cover classes, and therefore tend to ignore those that have very low frequencies of occurrence (Richard 1993). In this study a cluster classification module from the IDRISI software was used. First a false color composite image (FCC) was produced from band 1, 2 and 4. As the intention was to uncover major land cover classes, a broad generalization level was chosen, revealing 5 classes in the two images.

5.2 Maximum likelihood classification

The Gaussian Maximum Likelihood algorithm is a supervised classifier, i.e. the analyst supervises the classification by identifying representative areas, so called training areas. These areas are then described numerically and presented to the computer algorithm which classifies the pixels of the entire scene into the respective spectral class that appears to be most alike. In a maximum likelihood classification the distribution of the response pattern of each class is assumed to be normal (gaussian). The training stage is important since its characteristics determine the outcome of the classification. The data should include all spectral variation within each class. In theory, a statistically based algorithm requires a minimum of n+1 pixels for training in each class, where n is the

number of wavelength bands. However, in practice, the use of a minimum of 10n to 100n is advised by Lillesand and Kiefer (1994).

Using the results of the unsupervised cluster classification a simple classification scheme of six classes (5 land cover classes and water) was worked out. The 1989 scene was classified taking training data for the six classes by the use of Horqin desertification/land use map and the field data. Between 5-10 training sites within each class distributed over the entire image were identified. These sites were chosen to represent the land cover classes described in Table 4. In all maximum likelihood classifications the four MSS bands as well as a computed NDVI (normalized difference vegetation index) were included.

Table 4. Classification scheme used for the maximum likelihood classification.

Image Classes	Corresponding class from Map of Desertification in Horqin Grassland	Corresponding field data class
moving sand	severe desertification: < 10 % vegetation cover	< 10 % vegetation cover
water	-	-
cultivated land	farmlands	cultivated non-irrigated and irrigated
grassland 10-60% cover	slight desertification: grassland 30-60 % cover, moderate desertification: 10-30 % cover	grassland 10-30 % cover grassland 30-60 % cover
grassland 60-100% cover	latent: > 60 % cover	grassland > 60 % cover
scrub forest	woodland	scrub forest

In the 1975 image the choice of training data in the absence of reliable ground data has to be considered somewhat subjective. A prerequisite for being able to compare the two images is the proximity in acquisition dates of the scenes. Initially the training file from the 1989 was overlaid on the 1975 FCC and the concordance was assessed. A limited number of training areas were useful for both classifications and remaining signatures were chosen visually through combining spectral, textural and contextual information. In the case of water and bare sand the identification of training areas was relatively easy. Agriculture land was in some cases easy delineated, but in river valleys, in the absence of structures indicating fields, some of the areas could in practice be natural vegetation of wetland character. The separation of the two different kinds of grassland becomes biased in the absence of maps or field data. However, the 1975 FCC, even clearer than the 1990 FCC, identified differences in spectral response, which seem to correspond with the two classes and which was also confirmed by the cluster classification in the northern part of the image.

Classification of digital images can result in rather speckled images with unnaturally inhomogeneous areas. A post classification filtering process was applied to clean up the images and produce more homogenous areas. Using a mode filter the most frequently

occurring DN-value within the filter window surrounding each pixel is computed. A 3x3 pixel mode filter window was applied in this study to clean the classified image to the generalization of the Horqin desertification map.

5.3 Visual interpretation and additional data used

A problem of the maximum likelihood classification occurred due to the similarity in reflectance characteristics of scrub forest and cropland, which resulted in an over-representation of cropland. Since the areas of scrub forests are situated on high elevation on relatively steep hill slopes in comparison to the cropland which is mainly located in the river valleys, a digital elevation model (1km spatial resolution) was used for separating these classes. The most suitable elevation boundary to separate scrub forests and cropland was found to be at 850 m.

By using contextual information and maps some manual editing was done to correct for obvious misclassification of cropland at the expense of grassland with a vegetation cover >60%. A limited number of areas apparently assigned to cropland instead of scrub forest were manually edited as well. The procedure here was to visually compare the FCC and the desertification/land use map and systematically check the result of the classification. Areas apparently mal classified were corrected.

5.4 Evaluation

In September 1996 a combined reconnaissance and ground data field visit was made to the central part of the Horqin steppe (Table 4). Ground cover data was collected for 140 points in the study area by sampling areas in connection to passable roads. These points were georeferenced by GPS. 36 points of these, which fell within the area analyzed in this study, were used for a preliminary evaluation. The evaluation of the 1989 image with the field data gave poor results. Most likely this is due to the time difference between image acquisition and field data but also a result of low precision when georeferencing the image. Another source of poor correspondence could be the sampling method, here so-called “road sampling”, which is an efficient method when covering large areas. The sampling was done in areas close to river systems, as this is where most of the farmland and therefore the roads are located, but where land use may undergo rapid changes. Because of the unknown degree of comparability the results of the field data evaluation are therefore not further presented here.

6. Results and discussion

The accuracy of the geometric correction map to image is satisfactory considering the scale, 1:500 000, used in the transformation. Because the correction image to image is within one pixel, reliable comparison is still possible between the different scenes. As discussed in section 5.4, the map scale is one of the obstacles for proper evaluation with field data.

The cluster classification, set to a broad generalization level, indicated separability between 5 classes (excluding water), which were visually compared to the desertification map (see Table 4 for class description). The results corresponded approximately with the classes, severe desertification, moderate desertification, slight desertification, latent desertification and finally a class including both farmland and woodland. It can be concluded that the cluster classification reveals a pattern that roughly conforms with the pattern of the desertification map, hence there is a significant spectral difference which follows the vegetation cover distribution. Separating the two mapped classes slight and moderate desertification was found difficult using vegetation indices based on MSS data (Bremborg 1996) and therefore they were merged in this study. The cluster classification also indicates the difficulty to separate cultivated area and woodland.

The radiometric correction was done according to well-established methodologies. However, differences in spectral response between the two years remain and it was not deemed possible to use the signature statistics from the 1989 image on the 1975 image. The training areas for the maximum likelihood classification were therefore chosen separately for the two time points according to section 5.2.

The results of the supervised maximum likelihood classifications prior to filtering and post classification editing are presented in Figure 5. In the 1975 image the pattern of land-use shows that most of the cultivated land is distributed around the Xiliao River system. The distribution of the different classes of vegetation cover shows a gradient of low vegetation cover next to the farmland along rivers or other water bodies, and also on the sandy plains, and increasing cover on the hill slopes.

At higher elevations of the Daxinganling Mountains, in the northwestern part of the study area, patches of scrub forest remain. Some areas of scrub forest and high cover grassland have obviously been misclassified as cropland. These areas are situated on high elevations in the western part of the study area as well as on grass plains in the eastern part. When turning to the 1989 image the broad picture of the land cover classes persists, although cultivated areas have increased significantly, while classes of higher vegetation cover have expanded on behalf of classes with low vegetation cover. Also here the same type of misclassification exists.

Figure 5. Land cover classification prior to filtering and post classification editing

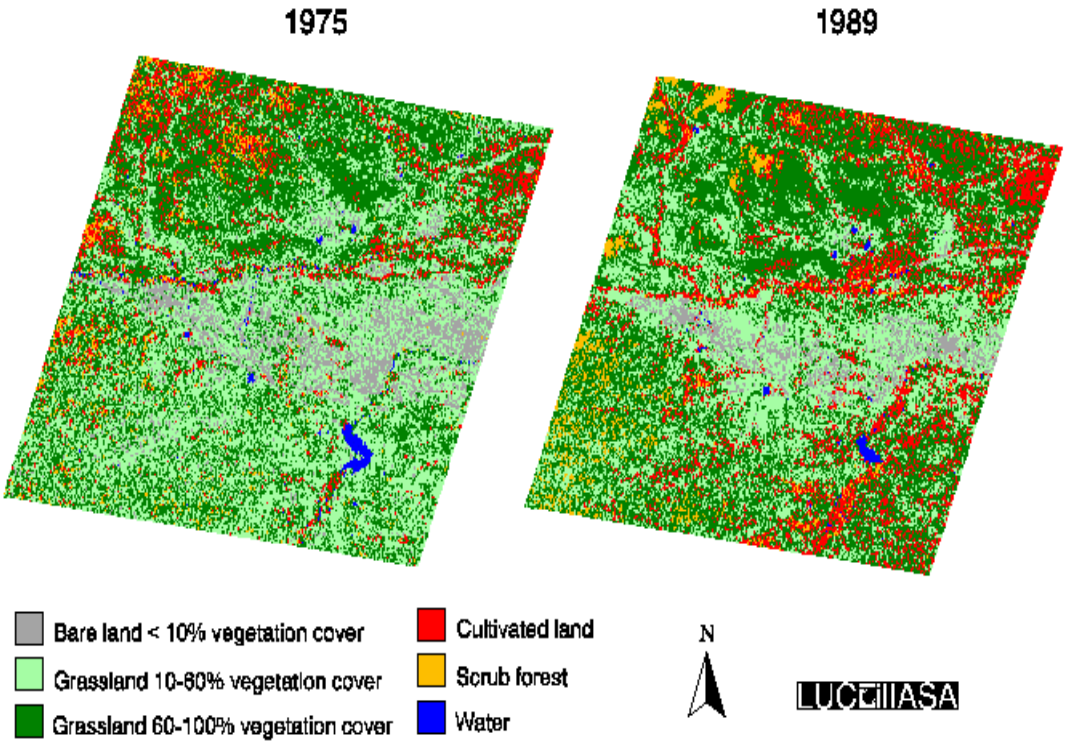

The results, after the use of the digital elevation model and the manual editing, are presented in figure 6. For better visualisation of the project area Figure 7 shows the final 1989 image once more, but now reclassifiied to a 400 m pixelsize and draped over a digital elevation model. Three main types of changes may be observed when comparing the class distribution between the two years.

First, larger areas of cultivated land are found in the 1989 image compared to 1975, mainly distributed around the Xiliao River system. Second, a large decrease of areas falling within the class “grassland 10-60% cover”, now assigned to “grassland 60-100 % cover”, is identified south of the sandy Xiliao River plain. Third, a decrease of sandy surfaces with the lowest vegetation cover, <10%, is found in the 1989 image.

Figure 6. Land Cover in 1975 and 1989 after manual corrections

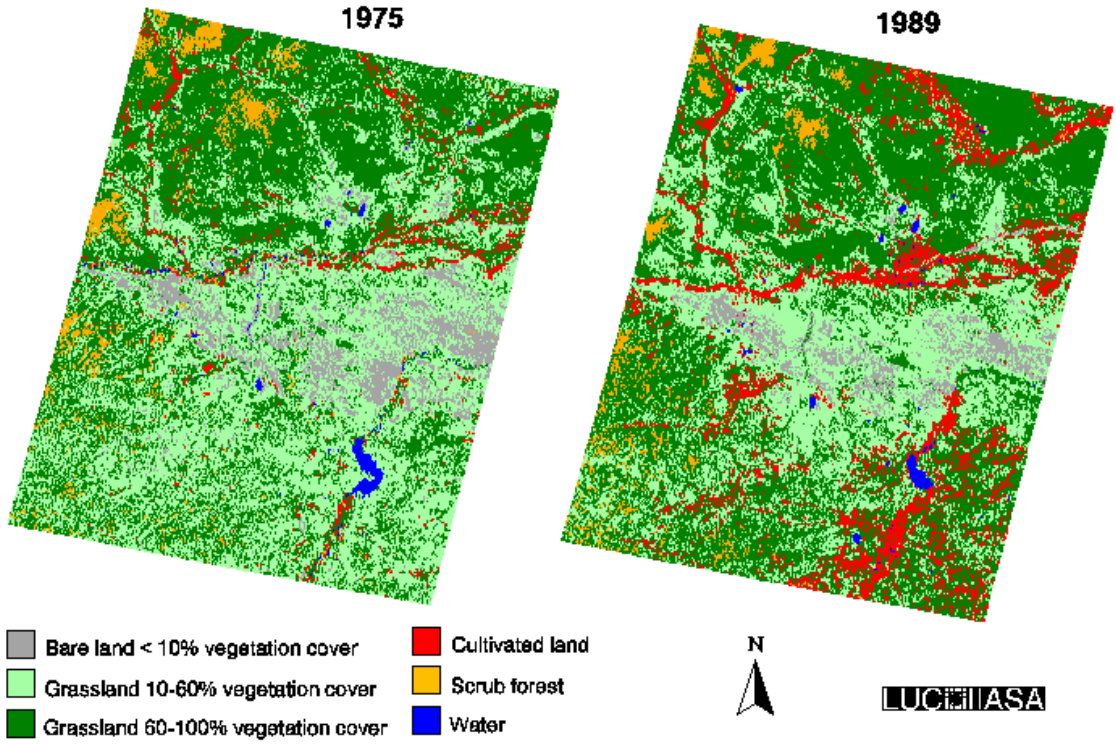

Figure 7. Land cover in 1989 reclassified to 400 m pixel size and draped over a digital elevation model

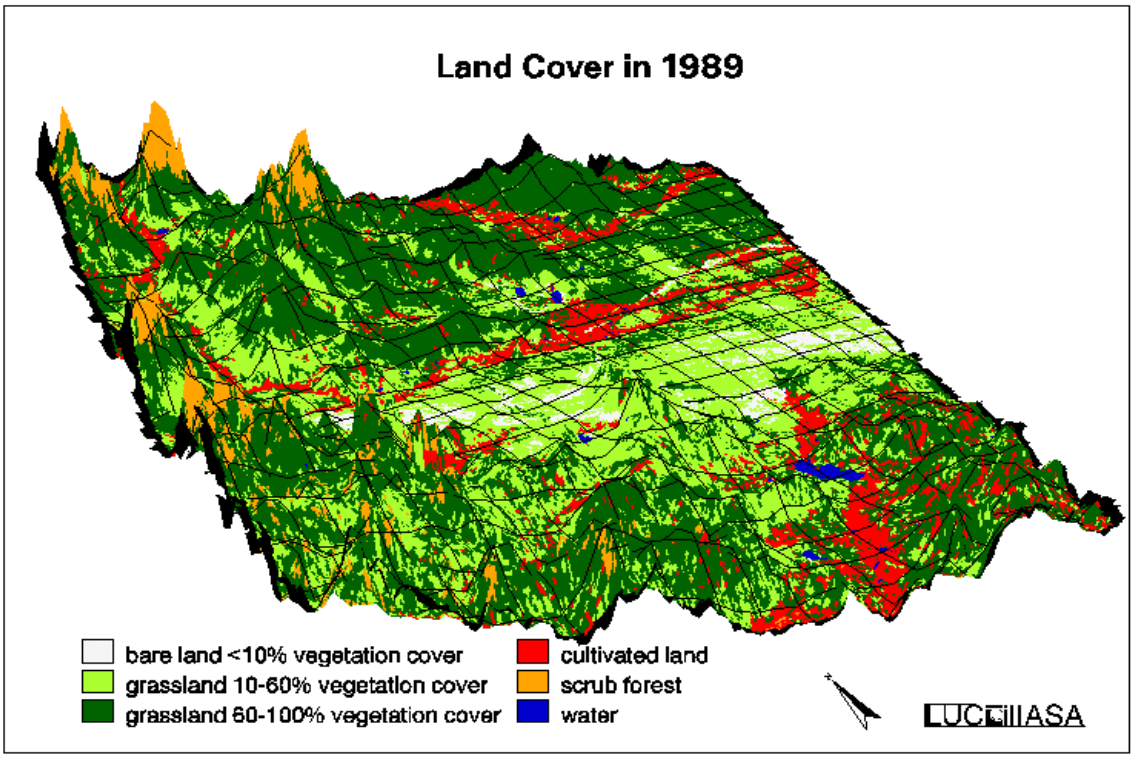

The percentage distribution of pixels to land-cover classes in the two years is visualized in figure 8. The lowest vegetation cover class (bare sand) has decreased from 6 to 3% and grassland with 10-60% cover has decreased from 45 to 33%. Increases occurred in the class grassland with 60-100% cover, namely from 42 to 51%, and in cultivated area which has increased from 3 to 11%.

Figure 8. The percentage distribution of pixels among the different land-cover classes of the final classification of the 1975 and 1989 image.

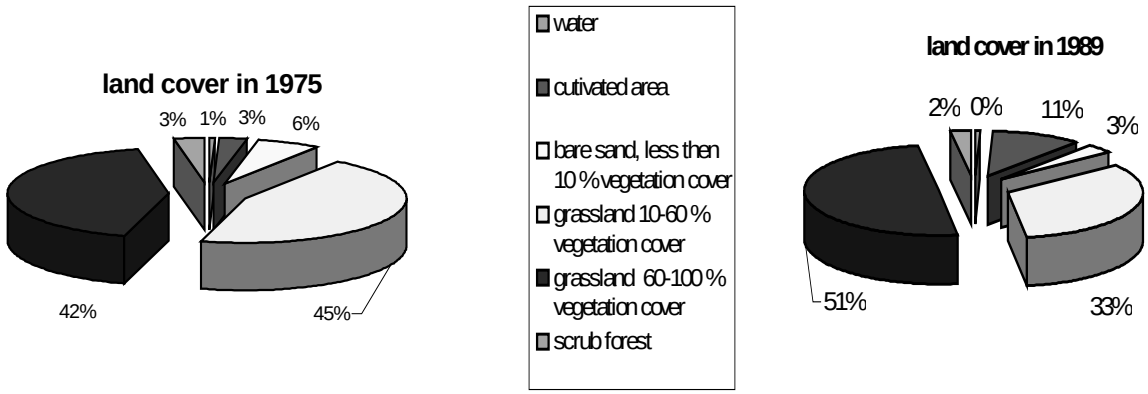

Looking into the actual direction of change in each pixel it can be seen that 60% (11673 km^2) of the project area show no changes in land cover (Table 5). The major changes in the remaining 40% of the area are grassland 10-60% in 1975 to grassland 60-100% in 1989 amounting to 3306 km^2. The increase in cultivated area stems obviously from both types of grassland, 988 km^2 from grassland 60-100% and 674 km^2 from grassland 10-60%. A relatively large area of 697 km^2 has apparently changed from bare land to grassland 10-60%.

Table 5. Distribution of Area of land-cover changes and area of no land cover changes between 1975 and 1989 (area in km^2).

Land cover changes			**No land cover changes**	
1975	**1989**	**area**		**area**
grass 10-60%	grass 60-100%	3306	grass 60-100%	5946
grass 60-100%	grass 10-60%	1178	grass 10-60%	4517
grass 60-100%	cultivated	988	bare land	497
bare land	grass 10-60%	697	cultivated	369
grass 10-60%	cultivated	674	scrub forest	286
scrub forest	grass 60-100%	268	water	58
grass 60-100%	scrub forest	140	*SUM of no changes*	11673
grass 10-60%	bare land	125		
cultivated	grass 60-100%	107		
other changes		311		
SUM of changes		7795		

7. Conclusions and further work

Lacking rigorous filed checks for 1975 and 1989, the following conclusions may be tentatively drawn. The distribution of land cover seems to be primarily determined by natural factors such as soil type, slope and elevation, and location of rivers and water holes. In addition to their obvious direct impacts, these also influence human activities and therefore indirectly affect land cover, for example through grazing pressure. The study shows a large expansion of cultivated areas mainly close to the river system, where irrigation may be used and where soil types are usually more suitable for cultivation. The increase of agricultural land around the river system is coherent with previous studies by Li (1990) indicating a major increase in agriculture land on the expense of good grassland. In this study the direction of land cover change is also from grassland to cropland, it seems however not to be confined to good grassland. Table 5 shows that 988 km^2 of the class 'grassland 60-100% vegetation cover' has been converted to cultivated land in comparison with 674 km^2 originating from the class 'grassland 10-60% vegetation cover'.

This study does not confirm any overall degradation of the area as far as concerns vegetation cover. On the contrary, the analysis implies a possible improvement of grassland. The overall area of the class 'grassland 60-100% vegetation cover' has increased from 42% of total area in 1975 to 51% in 1989. Especially in the loess area south of the Xilao River, the class 'grassland '10-60% vegetation cover' was replaced by the class 'grassland 60-100% vegetation cover'. Lower vegetation cover in 1989 compared to 1975 could only be detected in some patches primarily in the northwestern part of the study area, especially around minor rivers and water wholes. The decrease of areas assigned to the classes 'bare land vegetation cover <10%' and 'grassland vegetation cover class 10-60%' can not directly be explained by the rainfall data. The rainfall data showed no trend of higher rainfall. Further analysis of a denser precipitation data net, as well as analysis of monthly precipitation data should be performed.

The classification performed in the study involved both computer assisted and visual techniques. Even though the final editing of the classification was done visually and this involves more subjective methods than the automated classification, the combination of automated and visual classification methods was considered to give the best results under the given circumstances. For further work, however, improved classification methodologies, e.g. stratifying the study area according to soil type will be considered. Applying a neural network classification, which better than conventional classifications accepts additional geographical data with non-gaussian distributions, for example soil and elevation data, could also improve the result (Civco 1993).

Without proper evaluation of the classification at least for the time point in 1989, results of this study must be considered preliminary. Two strategies could be pursued to improve the evaluation: (i) adding two other images to allow comparison with recent field data, and (ii) performing an evaluation of the 1989 classification by systematically selecting points on the Desertification/land use map. Further work in case study areas with higher

resolution SPOT/Landsat TM images will also make it possible to identify expansion/reduction of small scale agriculture in the dune area in the center of the Xiliao River plain and on the hill slope grassland, as well as detecting smaller erosion features. The difficulty of tackling the natural high variability in semi-arid environments remains. Interpretation of an additional scene, already at hand for 1984, will improve vegetation cover assessment over time. Finally, using high temporal resolution NOAA satellite data would give further indication of changes in vegetation cover and biomass for the period after 1981, from which such data is available.

References

Ahlcrona, E., 1988. The impact of climate and man on land transformation in central Sudan, applications of remote sensing. Ph.D. Thesis. Meddelanden från Lunds Universitets Geografiska Institutioner. Avhandlingar 103. Lund University Press: Lund.

Bremborg, P., 1996. Desertification mapping of Horqin Sandy Land. Inner Mongolia, by means of remote sensing. M.S. Thesis. Seminarieuppsatser 38. Department of Physical Geography, Lund University.

Civco, D. L., 1993. Artificial neural networks for land-cover classification and mapping. International Journal of Geographical Information Systems, 7 (2). 173-186.

Fischer G., Y. Ermoliev, M. A. Keyzer, and C. Rosenzweig, 1996. Simulating the socio-economic and biogeophysical driving forces of land–use and land-cover change: The IIASA land-use change model. WP-96-010, International Institute for Applied systems Analysis, Laxenburg, Austria.

Hall-Kynöves, K., 1988. Remote sensing of cultivated lands in the south of Sweden. Ph.D. Thesis. Meddelanden från Lunds Universitets Geografiska Institutioner. Avhandlingar 102. Lund University Press: Lund.

Hoffer, R. M., 1978. Biological and Physical considerations in applying computer-aidede analysis techniques to remote sensor data. In Remote sensing: The quantitative approach. (Ed. by Swain R.H. and Davis, S. M.). McGraw-Hill, New York.

Lanzhou Institute of Desert Research, 1991, *Map of Land Desertification in Horqin Grassland, 1:500 000*, Academia Sincia, Chengdu Cartographic Publishing House**.**

Li Yuchen, 1990, Sandification process of Horqin Sandy Land and its comprehensive treatment. Proceedings, International conference on Grassland Science. Hohhot.

Lillesand, T. M. and Kiefer, R. W., 1987. Remote sensing and image interpretation. John Wiley and sons: New York.

Luk, S-H., 1983. Recent trends of desertification in the Maowusu Desert, China. Environmental Conservation, 10 (3). 213-223.

Longworth, J. and Williamson, G., 1993. China's pastoral region. Cambridge: University Press.

Ma, C. and Chang, S., 1980. It is of immediate urgency to protect our environmant and natural resources. Economic Management, 10, 28-39.

Markham, B. L. and Baker J. L., 1986. Landsat MSS and TM post-calibration dynamic ranges, Exoathmospheric reflectances and at-satellite temperatures. EOSAT. Landsat Technical notes, No.1.

National research council, 1992. Grasslands and grassland sciences in northern China: A report of the scholary communication with the People's Republic of China. Washington, D.C.: National academic press.

Rasmussen, K., 1993. Status on satellite remote sensing of environmant and agriculture in African Drylands. Proceedings, Seminar on satellite remote sensing of environment and agriculture in developing countries. Institute of Geography, University of Copenhagen, Denmark.

Richards, J. A., 1993. Remote sensing digital image analysis, an introduction. Springer-Verlag: Berlin.

Sheey, P. S., 1992. A perspective on Desertification of Grazingland Ecosystem in North China. Ambio, 21. 303-307.

Smil, V., 1987. Land degradation in China. Pp. 214-222 in Land degradation and society. (Ed. Blakie, P. and Brookfield, H.). London: Routhledge.

Zhu, Z., Di, X., Chen, G., Zou, B., Wang, K., and Zhang, J., 1988. Desertification and rehabilitation, case study in Horqin Sandy Land. Institute of Desert Research. Academia Sincia. Lanzhou.

Zhao, X., 1992. Litter decomposition in Naiman, Inner Mongolia, China, in relation to climate and litter properties. Sveriges Lantbruksuniversitets Rapporter 55.

Personal communication

Zhao, Xeuyoung. Institute of Desert Research, Chinese Academy of Sciences, 730000 Lanzhou, China.